Macromolecules **2005,** *38,* 2999−3006

Microphase Separation in Ultrathin Films of Diblock Copolymers with Variable Stickiness of One of the Blocks to the Surface

Igor I. Potemkin*,† **and Martin Möller**‡

Physics Department, Moscow State University, Moscow 119992, Russia, and Institut für Technische Chemie und Makromolekulare Chemie, RWTH Aachen, D-52062 Aachen, Germany

Received November 23, 2004; Revised Manuscript Received January 20, 2005

ABSTRACT: Surface interaction controlled microphase separation leading to the formation of a chemically heterogeneous surface nanopatterns in dry ultrathin films of *A*−*B* diblock copolymers is studied theoretically in the strong segregation limit. On a planar surface one of the blocks (*A* block) is strongly adsorbed, forming a tightly bound monomolecular layer (two-dimensional melt). Interaction of the second block (*B* block) with the surface can be varied from the strong attraction (two-dimensional conformation) to the strong repulsion (three-dimensional conformation) including regime of the weak interaction. Because of the strong incompatibility of *A* and *B* monomer units, chemically heterogeneous surface pattern can emerge. Depending on the block length ratio and on interaction parameters, various microstructures can be formed. They comprise surface micelles with prominent or flat disklike core, parallel stripes, and holelike micelles of monomer thick core and prominent corona (inverse disklike structure). The main geometrical parameters of the structures such as the size of the core and the period are determined as functions of the lengths of the blocks and of the interaction parameters.

1. Introduction

Generation of a chemically heterogeneous surface pattern by the controlled adsorption and self-assembly of block copolymers in microdomains represents a topical challenge for functional substrates and templates in nanotechnology, molecular biology, biomineralization, colloid science, and supramolecular chemistry.[1−13] One of the ways to design heterogeneous surfaces is based on preparation of relatively thin films comprising few periods of the bulk microstructure. It is well-known that the shape of the microdomains is primarily controlled by the relative length of the constituent blocks.[14−16] Proximity of the macroscopic phase boundaries introduces orientation of the microdomains and brings influence to the film structure as well. The key parameters, which govern the orientation, are the interfacial energies of the boundaries[17,18] and the film thickness.[19] If one of the blocks has a lower surface tension than the other one, it covers the film surface, and in the case of lamellar structure the film surface is unstructured.[20] In particular, parallel orientation of the lamellae to the substrate was observed in thin films of a symmetrical polystyrene-*block*-poly(methyl methacrylate) on a SiO_2 substrate.[7] Recent experiments with symmetrical polystyrene-*block*-polybutadiene on SiO_2[19] showed that perpendicular orientation of the lamellae can be stable if the polymer has a high molar mass. In this system, none of the blocks have a strong affinity toward the substrate or the air. Many other factors such as electric field,[18] competition of nonlamellar bulk morphology with the affinity of the blocks to the surface,[21] and chemically patterned substrates[22] can also have a strong influence on the orientation of the diblock copolymer domains.

A different strategy for reliable preparation of a chemically heterogeneous surface pattern is based on ultrathin films whose thickness is much less than the equilibrium period of the bulk morphology. One of the ways to obtain such films is the adsorption of a polystyrene-*block*-poly(2,4-vinylpyridine) diblock copolymer (PS-*b*-P2,4VP) on mica from a dilute solution.[23−27] In this case, the strongly adsorbed P2,4VP blocks wet the mica surface as an ultrathin, approximately monomer thick polymer layer whereby the blocks become largely extended. The PS blocks dewet both the P2,4VP layer and mica. They aggregate to surface clusters atop the P2,4VP layer in order to minimize the number of unfavorable contacts with the polar blocks and the air. Detailed experiments and scaling analysis of the surface-induced nanopatterns (SINPAT) showed that the heterogeneous surface structure is stable in a very wide range of block lengths.[26−29] When aggregated blocks (PS) are not so long, spherical clusters ordered with the symmetry of hexagonal lattice are more favorable. For longer PS blocks a stripelike structure is formed.[26,29]

The described above ultrathin films can be attributed to the systems with the so-called sticky (P2,4VP)−nonsticky (PS) toward the substrate copolymers. On the other hand, there are copolymers where the stickiness of one of the blocks can be variable. For instance, poly(ethylene oxide)-*block*-poly(2-vinylpyridine) (PEO−P2VP) on mica is an example of the sticky−sticky copolymer. The ability of water-soluble PEO blocks to desorb in a water environment relegates them to the sticky−nonsticky copolymers as well. Another example of copolymer with variable stickiness is a molecule having associating groups in the nonsticky block. For such groups, attraction to the surface can be "switched on" or "switched off" by external fields. For instance, photosensitive groups are spiropyrane substituents which can be switched from a nonionic to zwitterionic state, i.e., switching the dipole moment by light.

Variation of the stickiness can result in the structural reorganization of the SINPAT. The present paper is directed to the theoretical study of microstructures in ultrathin films of diblock copolymers obtained under variation of the stickiness of one of the blocks. We will develop a strong segregation theory for the analysis of possible morphologies of the film.

---

† Moscow State University.

‡ Institut für Technische Chemie und Makromolekulare Chemie.

* To whom correspondence should be addressed. E-mail igor@polly.phys.msu.ru.

10.1021/ma047576j CCC: $30.25

2. Model

Let us consider a dry, ultrathin film of $A-B$ diblock copolymers which is formed by adsorption of the blocks on a flat surface from a dilute solution.[23-26] A typical procedure of preparation of ultrathin films comprises dipping of the substrate in the solution and pulling it out. Therefore, we assume that the number of macromolecules on the surface is fixed and that the area of the surface is larger than the total area of the adsorbed segments. This assumption allows us to analyze all possible morphologies obtained via variation of the spreading parameter, i.e., of the film area. We suppose that the blocks are flexible and have statistical segments of equal length a; N_A and N_B are the numbers of the segments of A and B blocks, respectively. Strongly flatten on the surface A blocks (sticky blocks) form a monomer thick layer. Thus, we consider them as two-dimensional and assume that the density of A monomer units on the surface corresponds to the case of a two-dimensional melt, ensuring a minimum of unfavorable contacts of A monomer units with the air. We assume that B blocks are strongly incompatible with the A blocks and possess variable stickiness: a conformation of each individual B block can be varied between that of completely adsorbed (two-dimensional) chain and of partially desorbed, "shrunken" chain. Such conformational variations are controlled by the interactions of B blocks with the surface. A competition of the interfacial interactions with the entropic elasticity of the blocks can lead to the lateral phase separation resulted in the formation of various microstructures. The type of the surface structure depends on the relative length of the blocks and on the interaction parameters. For the described system, we will examine the conditions for the stability of (i) hexagonally packed micelles with a disklike core formed by partially desorbed B blocks ("islands" in a "see" of A blocks), (ii) parallel stripes, and (iii) hexagonally packed, disklike "holes" formed by strongly adsorbed A blocks in the matrix of partially desorbed B blocks (inverse disklike structure) (Figure 1a–c). Also, microphase separation of completely adsorbed (2D) chains will be considered. The analysis will be done within the strong segregation approximation.[15]

2.1. Disks. The disklike micelle is modeled as that having dense, disklike core of the thickness h and of the radius R formed by B blocks. We will study mainly the regime of weak desorption of the B blocks when the end-to-end distance of them is considerably larger than the thickness of the core, $a \leq h \ll R$. In this regime a smoothed profile of the core can be approximated by a steplike one (Figure 1d). Strongly adsorbed A blocks occupy a ring of the thickness a and of the outer radius R_0 (the radius of the Wigner–Seitz cell). The free energy of the micelle can be written as a sum of four terms:

$$F_{\text{disk}} = F_{\text{int}} + F_{el}^{A} + F_{el}^{B} + F_{\text{conf}} \qquad (1)$$

The first term, F_{int}, is an interfacial energy. Its effect is to minimize the number of unfavorable contacts of monomer units of different blocks with each other and with the surrounding media:

$$F_{\text{int}} = (\gamma_{As} + \gamma_{Aa})\pi({R_0}^2 - R^2) + (\gamma_{Bs} + \gamma_{Ba})\pi R^2 + \gamma_{Ba}2\pi R(h - a) + \gamma_{AB}2\pi Ra + \gamma_0(\sigma_0 - \pi {R_0}^2) \qquad (2)$$

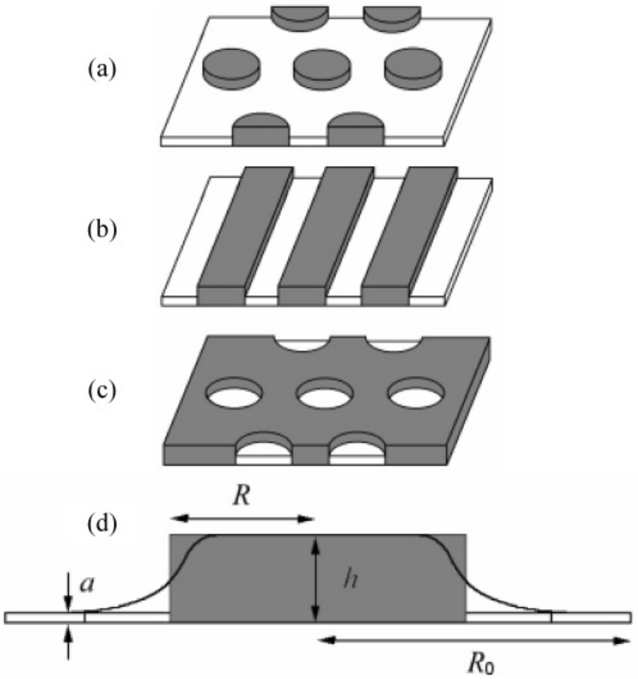

Figure 1. Schematic representation of microstructures formed by $A-B$ diblock copolymers with strongly adsorbed A blocks (white) and partially desorbed B blocks (gray): (a) disklike micelles ordered with the symmetry of hexagonal lattice; (b) parallel stripes; (c) holes ordered with the symmetry of hexagonal lattice (inverse disklike micelles). (d) A smoothed profile of the core comprising B blocks is modeled to be steplike in shape.

Here the first term is the energy of interactions of the A blocks with the substrate and with the air; γ_{As} and γ_{Aa} are the corresponding surface tension coefficients. The next two terms describe interactions of B blocks with the air and with the substrate. The fourth term is the energy of the $A-B$ interface. The last term in eq 2 corresponds to the energy of the substrate–air surface; σ_0 is the area of the substrate divided by the number of the micelles. This contribution is required in order to describe the spreading of B blocks on the surface. (This term is not a constant as it would be in the case of the fixed value of the area of the film.) Each micelle comprises Q chains. The condition for the dense packing of monomer units in the core and in the shell of the micelle can be written as follows:

$$\pi R^2 h = QN_B a^3, \quad \pi({R_0}^2 - R^2)a = QN_A a^3 \qquad (3)$$

where the volume per monomer unit is assumed to be equal to the cube of the segment length. Using above expressions, the interfacial energy per chain takes the following form:

$$\bar{F}_{\text{int}} = \frac{F_{\text{int}}}{Qk_{\text{B}}T} = \frac{2N_B a}{R}\Big(\bar{\gamma}_{Ba} + (\bar{\gamma}_{AB} - \bar{\gamma}_{Ba})\frac{a}{h}\Big) - \frac{N_B a}{h}S_B - N_A S_A + \frac{\bar{\gamma}_0\sigma_0}{Qa^2}$$

$$= \frac{2N_B a}{R}\Big(\bar{\gamma}_{Ba} + (\bar{\gamma}_{AB} - \bar{\gamma}_{Ba})\frac{a}{h}\Big) - \frac{N_B a}{h}S_B + \text{const} \qquad (4)$$

Here $\bar\gamma_i$, $i = Ba$, ..., are dimensionless surface tension coefficients, $\bar\gamma_i = \gamma_i a^2/k_BT$; S_A and S_B are dimensionless spreading parameters, $S_A = (\gamma_0 - \gamma_{As} - \gamma_{Aa})a^2/k_BT$, $S_B = (\gamma_0 - \gamma_{Bs} - \gamma_{Ba})a^2/k_BT$. They control the stickiness of the blocks. The blocks tend to be spread on the substrate to minimize substrate/air contacts when the spreading parameters are positive. Otherwise, the contacts of the blocks with the substrate are unfavorable. In our model S_A is positive and has to have a high enough value to provide a monomer thick layer. We will consider variation of the stickiness of B blocks assuming that the value of S_A is fixed. In the system with a fixed number of chains, the parameter σ_0/Q (the area of the substrate divided by the number of chains) is constant. That is why we denote the last two term in eq 4 as a constant which is the same for all kinds of microstructures which will be examined. The terms F^A_{el} and F^B_{el} in eq 1 are the free energies of radial stretching of A and B blocks. By analogy with the Semenov approximation for the micelles in the bulk,[15] we suppose that the free ends of A blocks are located at the boundary of the Wigner–Seitz cell. The elastic free energy per chain can be written as

$$\bar F^A_{el} = \frac{F^A_{el}}{Qk_BT} = \int_R^{R_0} \mathrm{d}r\, \frac{E(r)}{a^2} \qquad (5)$$

where the local stretching of the block $E(r) = \mathrm{d}r/\mathrm{d}n$ (derivative of the radial coordinate, r, $R < r < R_0$, with respect to the number of monomer units, n) depends on the coordinate. This dependence can be found from the condition of dense packing of A monomer units: a thin ring of the width dr contains Q dn monomer units so that $2\pi r\ \mathrm{d}r = Q\ \mathrm{d}n\ a^2$. Therefore

$$\bar F^A_{el} = \int_R^{R_0} \mathrm{d}r \frac{Q}{2\pi r} = \frac{Q}{2\pi}\ln\left(\frac{R_0}{R}\right) = \frac{R^2 h}{4N_B a^3}\ln\left(1 + \frac{N_A}{N_B}\frac{h}{a}\right) \qquad (6)$$

where the space-filling conditions, eq 3, are used. To calculate the elastic free energy of B blocks, the radial distribution of the free ends has to be taken into account. This term can be approximated by that obtained for the case of cylindrical micelles in the bulk:[15]

$$\bar F^B_{el} = \frac{\pi^2}{24}\frac{R^2}{N_B a^2} \qquad (7)$$

The last term in eq 1 is a loss of conformational entropy of the chains due to adsorption (confinement free energy). It comprises two parts: the free energies of A and B blocks. The confinement free energy of A blocks is constant for all types of the structure and therefore can be omitted. The free energy of B blocks can be calculated as that of the chain placed in a slit of the thickness h. Owing to the condition $R \gg h$, we can use the so-called ground-state approximation[30] where the energy per monomer unit is the minimum eigenvalue λ of the differential equation:

$$\frac{a^2}{6}\frac{\partial^2\psi(x)}{\partial x^2} + \lambda\psi(x) = 0, \quad \frac{\partial\psi(x)}{\partial x}\Big|_{x=\pm h/2} = 0, \quad -\frac{h}{2} \le x \le \frac{h}{2} \qquad (8)$$

The boundary conditions at the surfaces of the slit ensure the constant density of monomer units throughout the slit. The solution of eq 8 is chosen from the condition that it should be symmetric with respect to the origin of coordinates (middle of the slit), i.e., $\psi(x) = \mathrm{const}\cdot\cos(x\sqrt{6\lambda}/a)$. Thus, the confinement free energy per chain takes the following form

$$\bar F_{\mathrm{conf}} = \frac{F_{\mathrm{conf}}}{Qk_BT} = N_B\lambda = \frac{2\pi^2}{3}\frac{N_B a^2}{h^2} \qquad (9)$$

Summation of all contributions to the total free energy results in

$$\bar F_{\mathrm{disk}} = \frac{F_{\mathrm{disk}}}{Qk_BT} = \frac{2N_B a}{R}\left(\bar\gamma_{Ba} + (\bar\gamma_{AB} - \bar\gamma_{Ba})\frac{a}{h}\right) + \frac{R^2}{4N_B a^2}\left(\frac{h}{a}\ln\left(1 + \frac{N_A}{N_B}\frac{h}{a}\right) + \frac{\pi^2}{6}\right) - \frac{N_B a}{h}S_B + \frac{2\pi^2}{3}\frac{N_B a^2}{h^2} \qquad (10)$$

where all constant terms are omitted. Minimizing $\bar F_{\mathrm{disk}}$ with respect to R, we get

$$\bar F_{\mathrm{disk}} = \frac{3}{2}\left[2N_B\left(\frac{h}{a}\ln\left(1 + \frac{N_A}{N_B}\frac{h}{a}\right) + \frac{\pi^2}{6}\right)\left(\bar\gamma_{Ba} + (\bar\gamma_{AB} - \bar\gamma_{Ba})\frac{a}{h}\right)^2\right]^{1/3} - \frac{N_B a}{h}S_B + \frac{2\pi^2}{3}\frac{N_B a^2}{h^2}$$

$$R = a\left[\frac{4N_B^{\,2}\left(\bar\gamma_{Ba} + (\bar\gamma_{AB} - \bar\gamma_{Ba})\frac{a}{h}\right)}{\frac{h}{a}\ln\left(1 + \frac{N_A}{N_B}\frac{h}{a}\right) + \frac{\pi^2}{6}}\right]^{1/3} \qquad (11)$$

It is seen that the first term in $\bar F_{\mathrm{disk}}$ is proportional to $N_B^{1/3}$ while the next two terms have a linear dependence on N_B. Therefore, if the values of S_B are not so small, $S_B \gg (\bar\gamma_{Ba}/N_B)^{2/7}$, we can use a perturbation theory for minimization with respect to h:

$$h \approx a\frac{4\pi^2}{3S_B}, \quad \text{at } S_B \le \frac{4\pi^2}{3}$$

$$\bar F_{\mathrm{disk}} = -\frac{3N_B S_B^{\,2}}{8\pi^2} + \frac{3}{2}\left[2N_B\left(\frac{4\pi^2}{3S_B}\ln\left(1 + \frac{N_A}{N_B}\frac{4\pi^2}{3S_B}\right) + \frac{\pi^2}{6}\right)\left(\bar\gamma_{Ba} + (\bar\gamma_{AB} - \bar\gamma_{Ba})\frac{3S_B}{4\pi^2}\right)^2\right]^{1/3} + \ldots \qquad (12)$$

Similarly to the single chain adsorption,[31] the thickness of the core of the micelle is controlled by the balance between adsorption and confinement. When the spreading parameter S_B exceeds the threshold value $4\pi^2/3$, B blocks adopt a two-dimensional conformation, and the total free energy possesses the following form

$$h = a, \quad \text{at } S_B \ge \frac{4\pi^2}{3}$$

$$\bar F_{\mathrm{disk}} = -N_B\left(S_B - \frac{2\pi^2}{3}\right) + \frac{3}{2}\left[2N_B\left(\ln\left(1 + \frac{N_A}{N_B}\right) + \frac{\pi^2}{6}\right)\bar\gamma_{AB}^{\,2}\right]^{1/3} \qquad (13)$$

Taking into account that the thickness of the adsorbed layer of one of the blocks is not dependent on the presence of the second block, we can conclude that the spreading parameter of strongly adsorbed A blocks, S_A, has to be larger than $4\pi^2/3$ to keep the blocks in the monolayer, $S_A > 4\pi^2/3$.

It is well-known[15] that aggregation of block copolymers into micelles occurs if the length of the blocks forming the core of the micelle exceeds some certain threshold value N_B^c, $N_B^c \ll N_A$. To estimate this value, we compare the free energy of nonaggregated chain with the free energy of the chain in the micelle. When B blocks do not aggregate, they form single globules whose shape is assumed to be a disklike as well. Therefore, the interfacial energy has the same form as that of eq 4 with a different space-filling condition, $\pi R^2 h = N_B a^3$. Both A and B blocks are not stretched in this case and the contributions of the elastic free energy can be neglected. The resulting free energy of nonaggregated chain can be written as

$$\bar{F}_{\text{homo}} = \begin{cases} -\dfrac{3N_B{S_B}^2}{8\pi^2} + 4\pi\sqrt{\dfrac{\pi N_B}{3S_B}}\left(\bar{\gamma}_{Ba} + (\bar{\gamma}_{AB} - \bar{\gamma}_{Ba})\dfrac{3S_B}{4\pi^2}\right), & S_B \le \dfrac{4\pi^2}{3} \\ -N_B\left(S_B - \dfrac{2\pi^2}{3}\right) + 2\sqrt{\pi N_{\mathrm{B}}}\bar{\gamma}_{AB}, & S_B > \dfrac{4\pi^2}{3} \end{cases} \tag{14}$$

Comparison of eq 14 with the corresponding expressions, eqs 12 and 13, gives the following equations for the determination of $N_B^c(N_A^c)$:

$$N_A = \frac{3S_BN_B}{4\pi^2}\left(\exp\left\{\frac{64\pi^2}{27}\sqrt{\frac{\pi N_B}{3S_B}}\left(\bar{\gamma}_{Ba} + (\bar{\gamma}_{AB} - \bar{\gamma}_{Ba})\frac{3S_B}{4\pi^2}\right) - \frac{S_B}{8}\right\} - 1\right), \quad S_B \le \frac{4\pi^2}{3}$$

$$N_A = N_B\left(\exp\left\{\frac{32\pi}{27}\sqrt{\pi N_B}\bar{\gamma}_{AB} - \frac{\pi^2}{6}\right\} - 1\right), \quad S_B > \frac{4\pi^2}{3} \tag{15}$$

2.2. Stripes. If the length of the aggregated B blocks is increased, the stripelike structure can be stable.[26] This structure is characterized by infinite, alternating A and B stripes having different or equal thickness (Figure 1b). As for the case of the disks, each A stripe is a monomer thick layer of the width $2(R_0 - R)$; $R_0 - R$ is the end-to-end distance of A blocks. The shape of the cross section of B stripes is modeled as an rectangle so that the stripe of the width $2R$ has a constant thickness h throughout. Such assumption is adequate, if the condition $R \gg h$ is kept. The total free energy of the stripes is calculated in a similar way as for the case of the disks (eq 10):

$$F_{\text{str}} = \frac{R^2}{N_Ba^2}\left(1 + \frac{N_A}{N_B}\frac{h^2}{a^2}\right) + \frac{N_Ba}{R}\left(\bar{\gamma}_{Ba} + (\bar{\gamma}_{AB} - \bar{\gamma}_{Ba})\frac{a}{h}\right) - \frac{N_Ba}{h}S_B + \frac{2\pi^2}{3}\frac{N_Ba^2}{h^2} \tag{16}$$

where the space-filling conditions $2a(R_0 - R) = qN_Aa^2$ and $2hR = qN_Ba^2$ are used; $q = Qa/L$ is the aggregation number per unit length of the stripe. The first term in eq 16 is the elastic free energy of uniformly stretched A and B blocks, $(R_0 - R)^2/a^2N_A + R^2/a^2N_B$. The next two terms are the interfacial energies. The last term is the confinement free energy of B blocks. Minimizing $\bar{F}_{\text{str}}$ with respect to R, we get

$$\bar{F}_{\text{str}} = \frac{3}{2}\left[2N_B\left(1 + \frac{N_A}{N_B}\frac{h^2}{a^2}\right)\left(\bar{\gamma}_{Ba} + (\bar{\gamma}_{AB} - \bar{\gamma}_{Ba})\frac{a}{h}\right)^2\right]^{1/3} - \frac{N_Ba}{h}S_B + \frac{2\pi^2}{3}\frac{N_Ba^2}{h^2}$$

$$R = a\left[\frac{{N_B}^2\left(\bar{\gamma}_{Ba} + (\bar{\gamma}_{AB} - \bar{\gamma}_{Ba})\dfrac{a}{h}\right)}{2\left(1 + \dfrac{N_A}{N_B}\dfrac{h^2}{a^2}\right)}\right]^{1/3} \tag{17}$$

Perturbation theory for minimization with respect to h gives

$$\bar{F}_{\text{str}} = \begin{cases} -\dfrac{3N_B{S_B}^2}{8\pi^2} + \dfrac{3}{2}\left[2N_B\left(1 + \dfrac{N_A 16\pi^4}{N_B 9{S_B}^2}\right) \times \left(\bar{\gamma}_{Ba} + (\bar{\gamma}_{AB} - \bar{\gamma}_{Ba})\dfrac{3S_B}{4\pi^2}\right)^2\right]^{1/3} + \ldots, & h \approx a\dfrac{4\pi^2}{3S_B}, \quad S_B \le \dfrac{4\pi^2}{3} \\ -N_B\left(S_B - \dfrac{2\pi^2}{3}\right) + \dfrac{3}{2}\,[2(N_A + N_B){\bar{\gamma}_{AB}}^2]^{1/3}, & h = a, \quad S_B > \dfrac{4\pi^2}{3} \end{cases} \tag{18}$$

This approach is valid for $S_B \gg (N_A\bar{\gamma}_{Ba}^2/N_B{}^3)^{1/8}$. One of the boundaries of the stability region of the stripelike structure is found by equating the free energies $\bar{F}_{\text{str}}$ and $\bar{F}_{\text{disk}}$:

$$1 + \frac{N_A}{N_B}\frac{16\pi^4}{9{S_B}^2} = \frac{4\pi^2}{3S_B}\ln\left(1 + \frac{N_A}{N_B}\frac{4\pi^2}{3S_B}\right) + \frac{\pi^2}{6}, \quad S_B \le \frac{4\pi^2}{3}$$

$$1 + \frac{N_A}{N_B} = \ln\left(1 + \frac{N_A}{N_B}\right) + \frac{\pi^2}{6}, \quad S_B > \frac{4\pi^2}{3} \tag{19}$$

2.3. Holes. With the increase of the length of partially desorbed B blocks one can expect that the holelike (inverse disklike) structure can be stable. This structure is characterized by a disklike, monomer thick core of A blocks and by thickened corona of B blocks (Figure 1c). Similarly to the free energy of the disks, eq 10, the free energy of the holes takes the form

$$\bar{F}_{\text{hole}} = \frac{R^2}{4N_Aa^2}\left(\frac{a}{h}\ln\left(1 + \frac{N_B}{N_A}\frac{a}{h}\right) + \frac{\pi^2}{6}\right) + \frac{2N_Ah}{R}\left(\bar{\gamma}_{Ba} + (\bar{\gamma}_{AB} - \bar{\gamma}_{Ba})\frac{a}{h}\right) - \frac{N_Ba}{h}S_B + \frac{2\pi^2}{3}\frac{N_Ba^2}{h^2} \tag{20}$$

where the space-filling conditions for the core of the radius R and for the corona of the radius R_0 are $\pi R^2 = QN_Aa^2$ and $\pi(R_0^2 - R^2)h = QN_Ba^3$, respectively. Minimizing $\bar{F}_{\mathrm{hole}}$ with respect to R and h, we get

$$h \approx a\,\frac{4\pi^2}{3S_B}, \quad S_B \leq \frac{4\pi^2}{3}$$

$$R = a\left(\frac{4{N_A}^2\left(\bar{\gamma}_{Ba} + (\bar{\gamma}_{AB} - \bar{\gamma}_{Ba})\frac{3S_B}{4\pi^2}\right)}{\frac{3S_B}{4\pi^2}\ln\left(1 + \frac{N_B}{N_A}\frac{3S_B}{4\pi^2}\right) + \frac{\pi^2}{6}}\,\frac{4\pi^2}{3S_B}\right)^{1/3}$$

$$\bar{F}_{\mathrm{hole}} = -\frac{3N_B{S_B}^2}{8\pi^2} + \frac{3}{2}\left[N_A\frac{32\pi^4}{9{S_B}^2}\left(\frac{3S_B}{4\pi^2}\ln\left(1 + \frac{N_B}{N_A}\frac{3S_B}{4\pi^2}\right) + \frac{\pi^2}{6}\right)\left(\bar{\gamma}_{Ba} + (\bar{\gamma}_{AB} - \bar{\gamma}_{Ba})\frac{3S_B}{4\pi^2}\right)^2\right]^{1/3} + \ldots \quad (21)$$

Monomer thick corona, $h = a$, is formed at $S_B > 4\pi^2/3$:

$$R = a\left(\frac{4{N_A}^2\bar{\gamma}_{AB}}{\ln\left(1 + \frac{N_B}{N_A}\right) + \frac{\pi^2}{6}}\right)^{1/3}$$

$$\bar{F}_{\mathrm{hole}} = -N_B\left(S_B - \frac{2\pi^2}{3}\right) + \frac{3}{2}\left[2N_A\left(\ln\left(1 + \frac{N_B}{N_A}\right) + \frac{\pi^2}{6}\right){\bar{\gamma}_{AB}}^2\right]^{1/3} \quad (22)$$

Conditions for the transition stripes−holes are found by equating the free energies $\bar{F}_{\mathrm{str}}$ and $\bar{F}_{\mathrm{hole}}$:

$$1 + \frac{N_B}{N_A}\frac{9{S_B}^2}{16\pi^4} = \frac{3S_B}{4\pi^2}\ln\left(1 + \frac{N_B}{N_A}\frac{3S_B}{4\pi^2}\right) + \frac{\pi^2}{6}, \quad S_B \leq \frac{4\pi^2}{3}$$

$$1 + \frac{N_B}{N_A} = \ln\left(1 + \frac{N_B}{N_A}\right) + \frac{\pi^2}{6}, \quad S_B > \frac{4\pi^2}{3} \quad (23)$$

If the length of B blocks exceeds some certain value, aggregation of A blocks into the micelles becomes unfavorable and homogeneous phase is formed. In this phase conformation of each individual chain can also be imagined as that of two-dimensional A block (monomer thick disk) surrounded by the 2D or partially desorbed B block (ring of the thickness a or h). Both blocks are not stretched, and the total free energy of the homogeneous phase takes the form

$$\bar{F}_{\mathrm{homo}} = \begin{cases} -\dfrac{3N_B{S_B}^2}{8\pi^2} + \sqrt{\pi N_A}\dfrac{8\pi^2}{3S_B}\left(\bar{\gamma}_{Ba} + (\bar{\gamma}_{AB} - \bar{\gamma}_{Ba})\dfrac{3S_B}{4\pi^2}\right), & S_B \leq \dfrac{4\pi^2}{3} \\ -N_B\left(S_B - \dfrac{2\pi^2}{3}\right) + 2\sqrt{\pi N_A}\bar{\gamma}_{AB}, & S_B > \dfrac{4\pi^2}{3} \end{cases} \quad (24)$$

Comparison of eq 24 with the corresponding expressions, eqs 21 and 22, gives the following equations for the order−disorder transition:

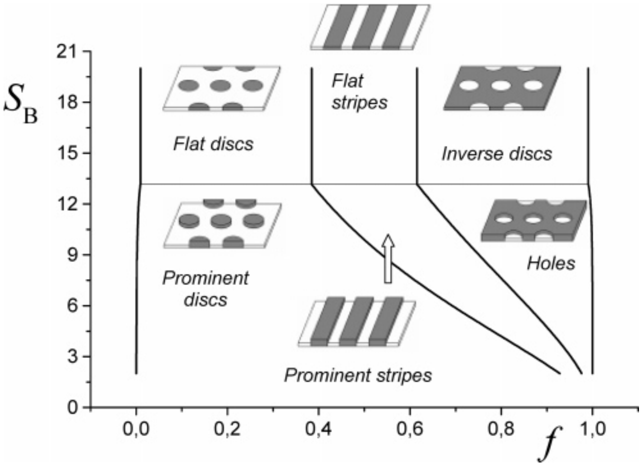

Figure 2. Phase diagram of the film in terms of the fraction of B monomer units $f = N_B/(N_A + N_B)$ and the spreading parameter S_B. The horizontal line $S_B = 4\pi^2/3$ splits the regions of flat and prominent morphologies. The spreading parameter S_A satisfies the inequality $S_A \geq 4\pi^2/3$ to ensure two-dimensional conformation of A blocks.

$$N_B = \frac{4\pi^2 N_A}{3S_B}\left(\exp\left\{\frac{16\pi^4}{9{S_B}^2}\left(\frac{32\pi}{27}\sqrt{\pi N_A}\left(\bar{\gamma}_{Ba} + (\bar{\gamma}_{AB} - \bar{\gamma}_{Ba})\frac{3S_B}{4\pi^2}\right) - \frac{S_B}{8}\right)\right\} - 1\right), \quad S_B \leq \frac{4\pi^2}{3}$$

$$N_B = N_A\left(\exp\left\{\frac{32\pi}{27}\sqrt{\pi N_A}\bar{\gamma}_{AB} - \frac{\pi^2}{6}\right\} - 1\right), \quad S_B > \frac{4\pi^2}{3} \quad (25)$$

3. Results and Discussion

The phase diagram of the film in terms of the fraction of B monomer units, $f = N_B/N$, $N = N_A + N_B$, and of the spreading parameter, S_B, is shown in Figure 2. This diagram is a solution of eqs 15, 19, 23, and 25. Both blocks are strongly adsorbed (monomer thick film) if S_B is above the value $4\pi^2/3$. In this case the diagram is symmetric with respect to the line $f = 1/2$. Similarly to diblock copolymers in the bulk, parallel stripes (an analogue of lamellar structure in 3D) are stable in the vicinity of $f = 1/2$. More asymmetric copolymers form flat disklike structures (monomer thick disklike core of A (B) blocks in the matrix of B (A) blocks). Homogeneous (disordered) film comprising nonaggregated blocks is stable only in the case of strongly asymmetric copolymers: $f \ll 1$ or $1 - f \ll 1$. The decrease of S_B below the value $4\pi^2/3$ results in partial desorption of B blocks, i.e., in the thickening of the film. Such asymmetry in interactions of A and B blocks with the substrate is responsible for a number of effects. First of all, aggregation of partially desorbed B blocks into the disks occurs at smaller values of f compared to the case of 2D blocks. This phenomenon is connected with the presence of excess polymer−air area which can be minimized by the aggregation. Prominent disks remain stable in very wide range of the values of f compared to the case of the monomer thick disks. Even long enough B blocks ($f > 1/2$) can form the core of the micelles. It becomes possible due to formation of the loops which decrease radial stretching of the B blocks. In other words, one can say that an ability of some of the segments to leave the substrate reduces the effective number of the segments

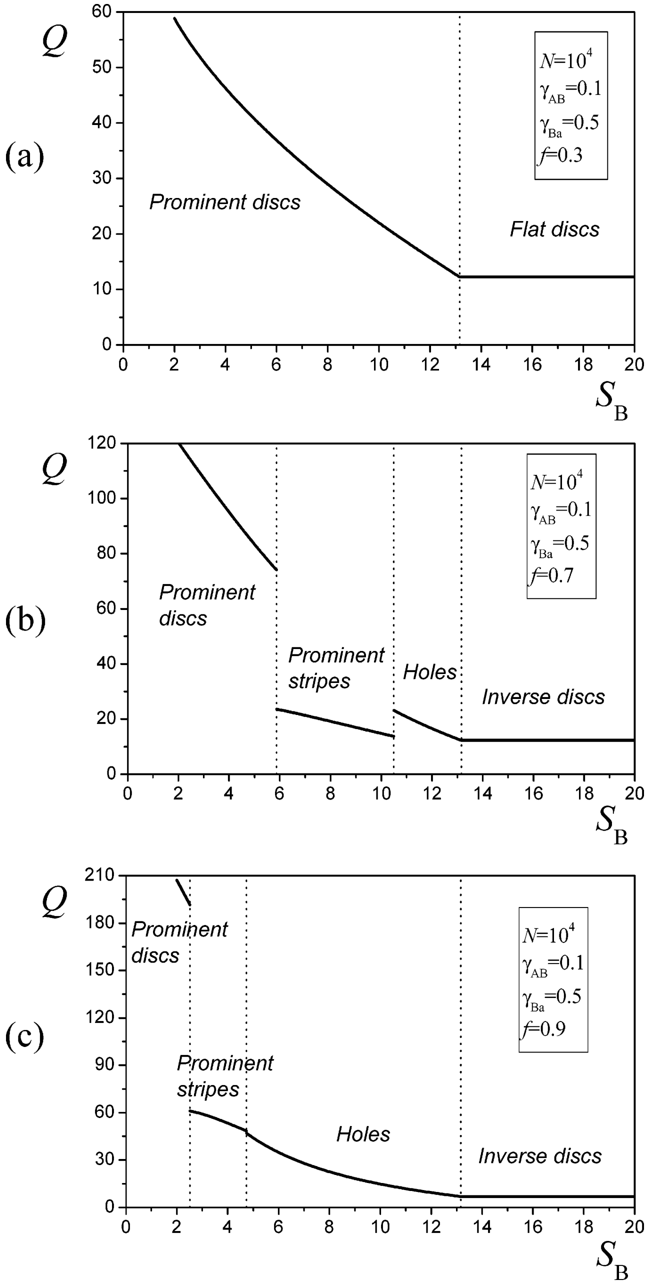

Figure 3. Aggregation number Q as a function of the spreading parameter S_B for different values of the fraction of B monomer units: $f = 0.3$ (a), 0.7 (b), and 0.9 (c). The vertical lines split the regions of stability of various microstructures. The aggregation number of the stripes is chosen to be $Q = q \cdot 2R/a$.

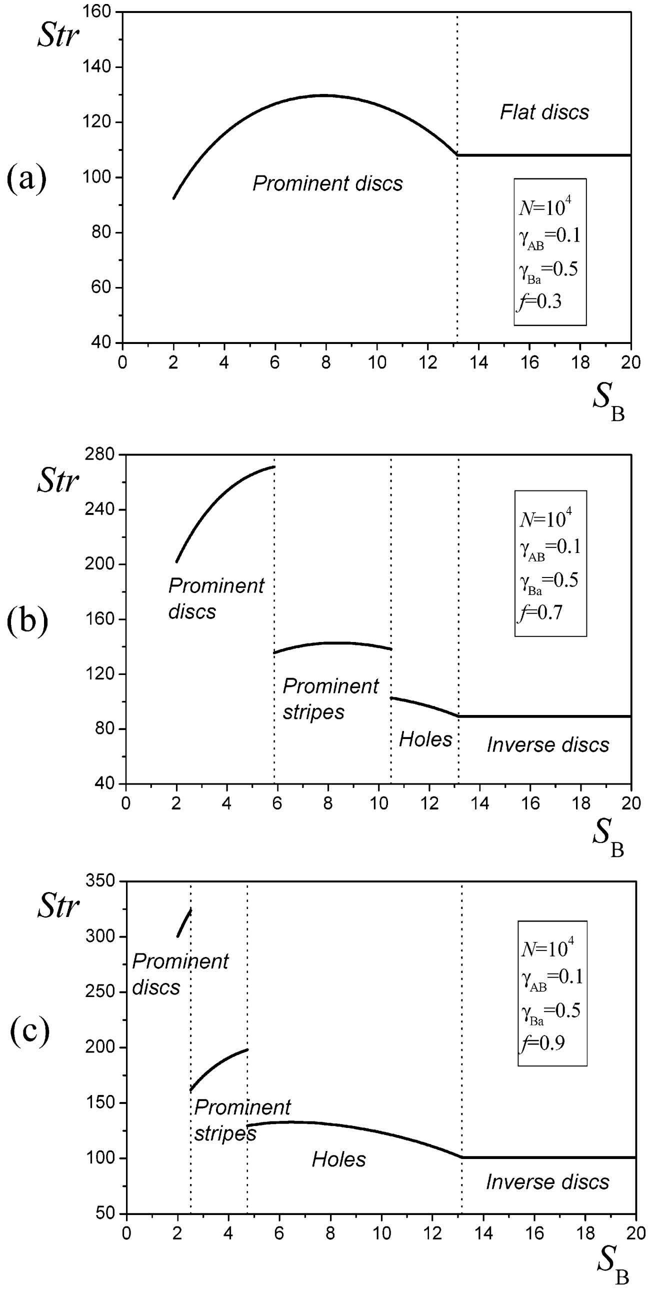

Figure 4. Characteristic stretching of B blocks Str as a function of the spreading parameter S_B for different values of the fraction f: $f = 0.3$ (a), 0.7 (b), and 0.9 (c). The stretching is defined as $Str = R/a$ for the disks and stripes and as $Str = (R_0 - R)/a$ for the holes and inverse disks.

in the block (the number of the segments located in the close vicinity of the substrate), $N_B^e = N_B a/h$, i.e., as if the partial desorption "shortens" the B blocks. On the other hand, the regions of stability of prominent stripes and holes narrow with the decrease of S_B (increase of h). This effect is a result of excess surface area with the air (compared to the flat structure). For example, thicker stripes have larger aggregation number (at fixed value of f) to minimize the area of the polymer–air interfaces (Figure 3). Therefore, the thicker stripes have higher elastic free energy which decreases at the transition into the holes. Note that the aggregation number is a decreasing function of S_B for all kinds of structures (Figure 3).

It is worth mentioning that the peculiar slope of the disks–stripes and stripes–holes boundaries in the phase diagram enables to manipulate microstructure of the film via variation of the spreading parameter at asymmetric composition of the copolymer. It can become promising for the making of multifunctional substrates where external stimuli can control the morphology. Characteristic stretching of the B blocks (R/a in the case of the disks and stripes and $(R_0 - R)/a$ in the case of the holes) as a function of the spreading parameter at fixed values of the composition of the copolymer is presented in Figure 4. Nonmonotonic behavior of R in the case of the disks is a result of the competition between two effects. First of all, the number of the adsorbed (effective) segments N_B^e is increased with S_B, leading to the increase of R. On the other hand, decreasing aggregation number acts in favor of the decrease of R. The effect of the aggregation number is

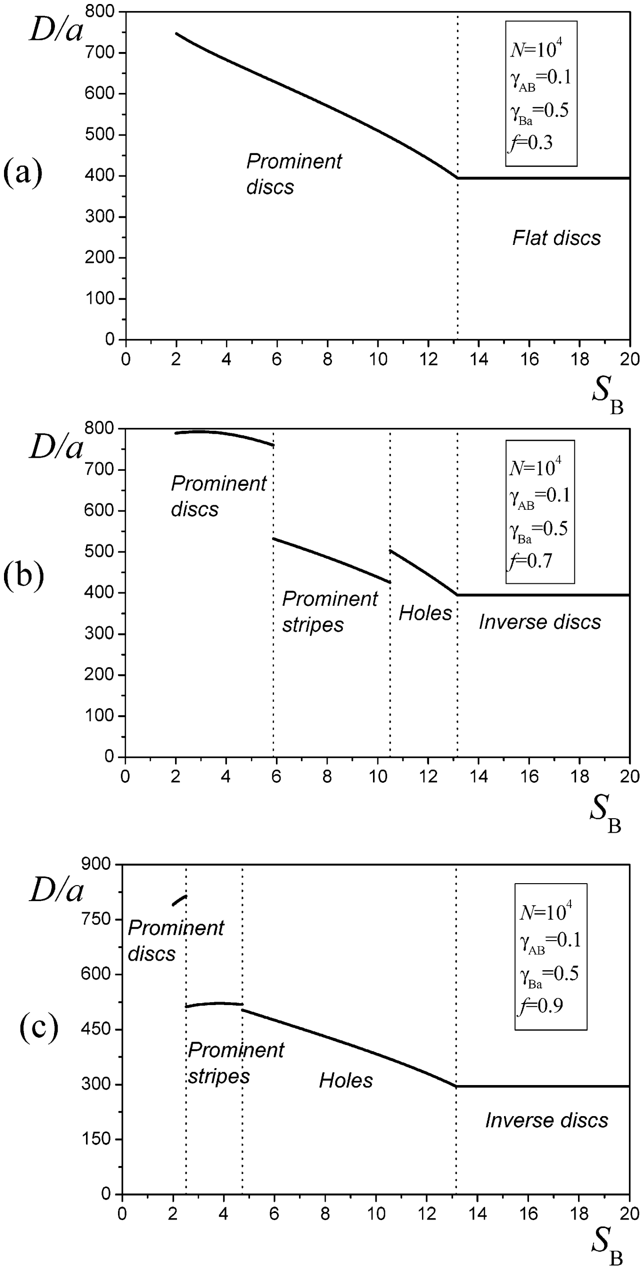

Figure 5. Period of the microstructure D as a function of the spreading parameter S_B. $f = 0.3$ (a), 0.7 (b), and 0.9 (c).

clearly seen in Figure 4 for the end-to-end distance of the B blocks in different structures: the stretching drops at the transition points. The behavior of the period of the structure, $D = 2R_0$, vs S_B is shown in Figure 5. It is seen that the disklike structure has a maximum period. Similarly to the case of diblock copolymers in the bulk, the size of the core of the surface microstructure scales with the number of segments in the core N_B (N_A) as $R \sim N_B^{2/3}$ ($N_A^{2/3}$); see eqs 11, 17, and 21.

Note that the above results obtained within the framework of the perturbation theory are valid for the regime of strong spreading of polymer B on the substrate: $S_B \gg (\bar{\gamma}_{Ba}/N_B)^{2/7}$ (for disks) and $S_B \gg (N_A\bar{\gamma}_{Ba}{}^2/N_B{}^3)^{1/8}$ (for stripes and holes). Weak interactions of polymer B with the substrate including wetting (positive values of S_B) and nonwetting (negative values of S_B), $|S_B| \ll (\bar{\gamma}_{Ba}/N_B)^{2/7}$ ($|S_B| \ll (N_A\bar{\gamma}_{Ba}{}^2/N_B{}^3)^{1/8}$), can also be analyzed if we use the initial expressions for the free energies, eqs 11 and 17. In this regime we can neglect the second term ($\sim S_B$) and use the condition $h \gg a$:

$$\bar{F}_{\text{disk}} \sim \left(N_B\bar{\gamma}_{Ba}{}^2\frac{h}{a}\right)^{1/3} + \frac{N_Ba^2}{h^2}, \quad |S_B| \ll (\bar{\gamma}_{Ba}/N_B)^{2/7}$$

$$\bar{F}_{\text{str/hole}} \sim \left(N_A\bar{\gamma}_{Ba}{}^2\frac{h^2}{a^2}\right)^{1/3} + \frac{N_Ba^2}{h^2}, \quad |S_B| \ll (N_A\bar{\gamma}_{Ba}{}^2/N_B{}^3)^{1/8} \quad (26)$$

Here all constants and logarithmic factors are omitted. Minimizing these free energies, we get

$$h_{\text{disk}} \sim a\left(\frac{N_B}{\bar{\gamma}_{Ba}}\right)^{2/7}, \quad R_{\text{disk}} \sim a\bar{\gamma}_{Ba}{}^{3/7}N_B{}^{4/7}$$

$$h_{\text{str/hole}} \sim a\left(\frac{N_B{}^3}{N_A\bar{\gamma}_{Ba}{}^2}\right)^{1/8}, \quad R_{\text{str/hole}} \sim a\left(\frac{N_B{}^3\bar{\gamma}_{Ba}{}^2}{N_A}\right)^{1/4} \quad (27)$$

The transition from the disks to the stripes occurs at $N_A \sim \bar{\gamma}_{Ba}{}^{2/7}N_B{}^{5/7}$ or $1 - f \sim (\bar{\gamma}_{Ba}/N_B)^{2/7} \ll 1$. We can see that in the regime of weak interactions of B blocks with the substrate the thickness h depends on N_B and N_A (stripes and holes). On the other hand, aggregation of the blocks makes them stretched so that $R \gg h$. In comparison with the regime of strong attraction of B blocks to the substrate, the parameter R_{disk} has a weaker dependence on N_B and R_{str} becomes dependent on N_A.

When repulsion of B monomer units with the substrate is strong, $S_B < 0$, $|S_B| \gg (\bar{\gamma}_{Ba}/N_B)^{2/7}$, or $|S_B| \gg (N_A\bar{\gamma}_{Ba}{}^2/N_B{}^3)^{1/8}$, there are two ways to minimize interfacial energy: (i) the B blocks can be detached from the substrate to aggregate atop the A blocks, or (ii) the B blocks minimize a contact area with the substrate via the thickening of the layers of polymer B. The first case is considered in our previous publications.[26–29] Here we estimate the parameters of the aggregates for the second case. Note that the contacts of polymer B with the substrate are energetically more favorable than the spreading atop the polymer A, if the spreading parameter of polymer B on the substrate is higher than that on the polymer A, i.e., if $\bar{\gamma}_{AB} + \bar{\gamma}_0 > \bar{\gamma}_{Aa} + \bar{\gamma}_{Bs}$. For the description of this regime, we neglect the last term ($\sim 1/h^2$) in eqs 11 and 17 and use the condition $h \gg a$:

$$\bar{F}_{\text{disk}} \sim \left(N_B\bar{\gamma}_{Ba}{}^2\frac{h}{a}\right)^{1/3} + \frac{N_Ba}{h}|S_B|, \quad |S_B| \gg (\bar{\gamma}_{Ba}/N_B)^{2/7}$$

$$\bar{F}_{\text{str/hole}} \sim \left(N_A\bar{\gamma}_{Ba}{}^2\frac{h^2}{a^2}\right)^{1/3} + \frac{N_Ba}{h}|S_B|, \quad |S_B| \gg (N_A\bar{\gamma}_{Ba}{}^2/N_B{}^3)^{1/8} \quad (28)$$

Minimizing these free energies, we get

$$h_{\text{disk}} \sim a\left(\frac{N_B}{\bar{\gamma}_{Ba}}\right)^{1/2}|S_B|^{3/4}, \quad R_{\text{disk}} \sim a\frac{(\bar{\gamma}_{Ba}N_B)^{1/2}}{|S_B|^{1/4}}$$

$$h_{\text{str/hole}} \sim a\frac{N_B{}^{3/5}}{N_A{}^{1/5}}\frac{|S_B|^{3/5}}{\bar{\gamma}_{Ba}{}^{2/5}}, \quad R_{\text{str/hole}} \sim a\frac{N_B{}^{3/5}}{N_A{}^{1/5}}\frac{\bar{\gamma}_{Ba}{}^{3/5}}{|S_B|^{2/5}} \quad (29)$$

where transition between the disks and stripes occurs at $N_B \sim N_A{}^2|S_B|^{3/2}/\bar{\gamma}_{Ba}$ or $1 - f \sim (\bar{\gamma}_{Ba}/N_B)^{1/2}/|S_B|^{3/4} \ll 1$. It is seen that in this regime $R \sim h$ for all kinds of structures and that the stretching of B blocks is negligible compared to the stretching of A blocks: $\bar{F}_{el}{}^B/\bar{F}_{el}{}^A \sim (\bar{\gamma}_{Ba}/N_B)^{1/2}/|S_B|^{3/4} \ll 1$ (for the disks), $\bar{F}_{el}{}^B/\bar{F}_{el}{}^A \sim \bar{\gamma}_{Ba}{}^{4/5}/(N_A{}^{3/5}N_B{}^{1/5}|S_B|^{6/5}) \ll 1$ (for the stripes), and $\bar{F}_{el}{}^B/\bar{F}_{el}{}^A \sim N_A{}^{1/5}\bar{\gamma}_{Ba}{}^{2/5}/(N_B{}^{3/5}|S_B|^{3/5}) \ll 1$ (for the holes). In our model the elastic free energy of B blocks was calculated at the assumption $R \gg h$, ensuring radial (longitudinal) stretching of the blocks. The neglect of $\bar{F}_{el}{}^B$ in the total free energy enables us to remove the restriction on h; i.e., the obtained estimation $R \sim h$ lies within the framework of the approach. Note that h and R in eqs 29 have the same exponents for N_A and N_B as in the case of the spreading of polymer B atop the polymer A.[26,28,29]

4. Conclusions

We have developed a strong segregation theory of microphase separation in ultrathin films of diblock copolymers obtained by strong adsorption of one of the blocks (A) on a plane surface. Surface interactions of B blocks are varied from the strong attraction (sticky blocks) to the strong repulsion (nonsticky blocks), including regime of the weak interactions. It was shown that both the chemical composition of the copolymer and the strength of interactions of polymer B with the surface control the morphology of the film. Chemically heterogeneous surface nanopatterns, which were calculated in this paper, comprise disk-, stripe-, and holelike structures depicted in Figure 1. The dependence of geometrical parameters of such structures on the block lengths was found. The most important prediction of the theory is that variation of the stickiness of one of the blocks can lead to the morphological changes.

Acknowledgment. The support of the Alexander von Humboldt Foundation (F. W. Bessel Research Award), the Deutsche Forschungsgemeinschaft within the SFB 569, and the Russian Foundation for Basic Research is gratefully acknowledged.

References and Notes

(1) Chou, S. Y.; Krauss, P. R.; Renstrom, P. J. *J. Vac. Sci. Technol. B* **1996**, *14*, 4129.
(2) Herminghaus, S.; Jacobs, K.; Mecke, K.; Bischof, J.; Fery, A.; Ibn-Elhaj, M.; Schlagowski, S. *Science* **1998**, *282*, 916.
(3) Spatz, J. P.; Roescher, A.; Sheiko, S.; Krausch, G.; Möller, M. *Adv. Mater.* **1995**, *7*, 731.
(4) Harrison, C.; Park, M.; Chaikin, P. *Polymer* **1998**, *39*, 2733.
(5) Park, M.; Harrison, C.; Chaikin, P.; Register, R.; Adamson, D. *Science* **1997**, *276*, 1401.
(6) Krausch, G. *Mater. Res. Rep.* **1995**, *14*, 1.
(7) Anastasiadis, S.; Russell, T. P.; Satija, S. K.; Majkrzak, C. F. *Phys. Rev. Lett.* **1989**, *62*, 1852.
(8) Bassereau, P.; Brodbreck, D.; Russel, T. P.; Brown, H. R.; Shull, K. R. *Phys. Rev. Lett.* **1993**, *71*, 1716.
(9) Thurn-Albrecht, T.; Steiner, R.; DeRouchey, J.; Stafford, C. M.; Huang, E.; Bal, M.; Tuominen, M.; Hawker, C. J.; Russell, T. P. *Adv. Mater.* **2000**, *12*, 787.
(10) Thurn-Albrecht, T.; Schotter, J.; Kästle, G. A.; Emley, N.; Shibauchi, T.; Krusin-Elbaum, L.; Guarini, K.; Black, C. T.; Tuominen, M. T.; Russell, T. P. *Science* **2000**, *290*, 2126.
(11) Boyen, H.-G.; Kastle, G.; Weigl, F.; Koslowski, B.; Dietrich, C.; Ziemann, P.; Spatz, J. P.; Riethmuller, S.; Hartmann, C.; Möller, M.; Schmid, G.; Garnier, M. G.; Oelhafen, P. *Science* **2002**, *297*, 1533.
(12) Haupt, M.; Miller, S.; Glass, R.; Arnold, M.; Thonke, K.; Möller, M.; Spatz, J. P. *Adv. Mater.* **2003**, *15*, 829.
(13) Böker, A.; Muller, A. H. E.; Krausch, G. *Polym. Mater. Sci. Eng.* **2001**, *84*, 312.
(14) Leibler, L. *Macromolecules* **1980**, *13*, 1602.
(15) Semenov, A. N. *Sov. Phys. JETP* **1985**, *61*, 733.
(16) Bates, F. S.; Fredrickson, G. H. *Annu. Rev. Phys. Chem.* **1990**, *41*, 525.
(17) Kellogg, G. J.; Walton, D. G.; Mayes, A. M.; Lambooy, P.; Russell, T. P.; Gallagher, P. D.; Satija, S. K. *Phys. Rev. Lett.* **1996**, *76*, 2503.
(18) Mansky, P.; Liu, Y.; Huang, E.; Russell, T. P.; Hawker, C. J. *Science* **1997**, *275*, 1458.
(19) Bush, P.; Posselt, D.; Smilgies, D.-M.; Rheinlander, B.; Kremer, F.; Papadakis, C. M. *Macromolecules* **2003**, *36*, 8717.
(20) Potemkin, I. I. *Macromolecules* **2004**, *37*, 3505.
(21) Turner, M. S.; Rubinstein, M.; Marques, C. M. *Macromolecules* **1994**, *27*, 4986.
(22) Tsori, Y.; Andelman, D. *Europhys. Lett.* **2001**, *53*, 722.
(23) Spatz, J. P.; Sheiko, S.; Möller, M. *Adv. Mater.* **1996**, *8*, 513.
(24) Spatz, J. P.; Möller, M.; Nöske, M.; Behm, R. J.; Pietralla, M. *Macromolecules* **1997**, *30*, 3874.
(25) Spatz, J. P.; Eibeck, P.; Mössmer, S.; Möller, M.; Herzog, T.; Ziemann, P. *Adv. Mater.* **1998**, *10*, 849.
(26) Potemkin, I. I.; Kramarenko, E. Y.; Khokhlov, A. R.; Winkler, R. G.; Reineker, P.; Eibeck, P.; Spatz, J. P.; Möller, M. *Langmuir* **1999**, *15*, 7290.
(27) Spatz, J. P.; Eibeck, P.; Mössmer, S.; Möller, M.; Kramarenko, E. Yu.; Khalatur, P. G.; Potemkin, I. I.; Khokhlov, A. R.; Winkler, R. G.; Reineker, P. *Macromolecules* **2000**, *33*, 150.
(28) Kramarenko, E. Yu.; Potemkin, I. I.; Khokhlov, A. R.; Winkler, R. G.; Reineker, P. *Macromolecules* **1999**, *32*, 3495.
(29) Eibeck, P.; Spatz, J. P.; Potemkin, I. I.; Kramarenko, E. Yu.; Khokhlov, A. R.; Möller, M. *Polym. Prepr. (Am. Chem. Soc., Div. Polym. Chem.)* **1999**, *40*, 990.
(30) Grosberg, A. Yu.; Khokhlov, A. R. *Statistical Physics of Macromolecules*; AIP Press: New York, 1994.
(31) Bouchaud, E.; Daoud, M. *J. Phys. (Paris)* **1987**, *48*, 1991.

MA047576J